©2020 Romanian Association of Nonconventional Technologies

DETERMINATION OF MICROHARDNESS AND DEPTH OF THERMALLY HARDENING ZONE IN QUALITY CARBON STRUCTURAL STEEL AFTER WEDM USING DIFFERENT DISCHARGE PARAMETERS

Vasyl Osypenko, Oleksandr Plakhotnyi, Oleksii Timchenko and Andrii Kondakov
Cherkasy State Technological University, Cherkasy, Ukraine osip5906@gmail.com, o.plakhotny@chdtu.edu.ua, alec.timchenko@gmail.com, kondakov.andrii@gmail.com

ABSTRACT: This article presents experimental studies of microhardness distributions along the depth of the thermally hardened zone in high-quality carbon Steel 45 (analog DIN 1.0503) after wire electrical discharge machining (WEDM) using a wide range of modes with known energy and time parameters of a single spark discharge. In the zone of thermal hardening of Steel 45 after WEDM were revealed extreme values of microhardness which exceed the maximum achievable at standard hardening of this grade of steel. In areas of ultrahigh hardness microcracks are absent. It is established that in WEDM of high-quality carbon steels with the use of discharge current pulses with energy and time parameters characteristic of modern EDM cutting machines, the current pulse duration has a dominant influence on the formation of the thickness of the thermally hardened layer. The amount of discharge energy released at the anode, within the parameters of the experiments, has a secondary effect on the machining process. The possibility of effectively influencing the formation of the necessary physical and mechanical properties of the surface layers of carbon steel parts with the help of time parameters of a single spark discharge is proved. It is proposed to use the obtained results to predict the thickness of the thermally hardened layer at WEDM of a wide group of structural and tool carbon steels. The established regularities expand the idea of the mechanisms of influence of time-energy characteristics of spark discharges on the formation of thermally hardened layer at WEDM of high-quality carbon steels and correlate well with the known research results in the field of electrophysical methods of materials machining.

KEYWORDS: wire electrical discharge machining, thermally hardened zone, microhardness, heat-affected zone.

1. INTRODUCTION

It has already become a classic approach, when the efficiency and quality of WEDM is evaluated by the parameters of microgeometry and the accuracy of the shape and size of the obtained surfaces [1, 2]. It is well known that the physical and mechanical properties, homogeneity, the structure and thickness of the heat-affected zone (HAZ) during processing by WEDM technology of steel surfaces significantly affect the performance properties of the part [3]. Depending on the operating conditions, the presence and parameters of the thermally hardened layer can play both a positive role [4, 5] and be an extremely undesirable consequence of WEDM because of thermal influence [6, 7]. Thus, the thermally hardened layer is one of the factors that determine the allowances, quantity and energy parameters of additional passes, or the use of finishing non-thermal technologies [8, 9].

In general, in WEDM of quality carbon steels and tool steels thermally hardened layer is characterized by the presence of hardened structures with high microhardness. The parameters of the HAZ are determined by the thermal processes in the zone of material removal of the part by the plasma of the discharge channel during machining. These indicators are complex functions of thermophysical characteristics of the material (density, heat capacity, thermal conductivity) which take into account their change with increasing temperature, discharge energy parameters (pulse duration, energy released at the anode, power density, its distribution on the contact spot and time) and heat transfer conditions after the collapse of the discharge channel.

In real technological conditions of WEDM, the most effective way to influence the formation of necessary operating conditions of physical and mechanical properties of surface layers of steel parts is possible by parameters of the generator of operating current. Based on the above, the purpose of this study is to replenish the database and expand ideas about the patterns of energy characteristics of process current pulses on the formation of the distribution of microhardness and thickness of the thermally hardened zone of WEDM of quality carbon steels.

2. EQUIPMENT AND MATERIALS

After analyzing a wide range of research results in this area, the methods and approaches described in [10] were used in planning and performing the experiments. To study the distribution of microhardness, 6 samples were made of high-quality carbon Steel 45 (analog DIN 1.0503) with dimensions of 100x20x20 mm. The samples were made by milling with an end mill diameter of 25 mm. Surface roughness after milling was Ra = 12 μm, deviation from flatness was not more than 0.13 mm. Roughness of the surface was studied using the

TIME 3221 profilometer and the DataView TIME3R Series software. Three base surfaces of 100x20 mm were grinded on each sample (for fixing on the machine and as a base for oblique grinding). The flatness inaccuracy on these surfaces was controlled using the coordinate measuring machine 3D CMM AXIOM CNC ABERLINK and did not exceed 0.003 mm. One surface 100x20 mm after milling (with a plastically deformed layer up to 0.1 mm thick) was left for WEDM.

To obtain surfaces formed by WEDM technology, a modern EDM machine AccuteX GE-43SA was used. Based on many years of research and calculations of energy characteristics of steel processing modes using this machine, the staff of the laboratory of electrophysical and electrochemical methods of materials processing Cherkasy State Technological University received data on a set of parameters of the main energy modes of the operating current generator. Fig. 1 shows an example of oscillograms of current and voltage of a single spark discharge when using the mode NQ0024 (Table 1).

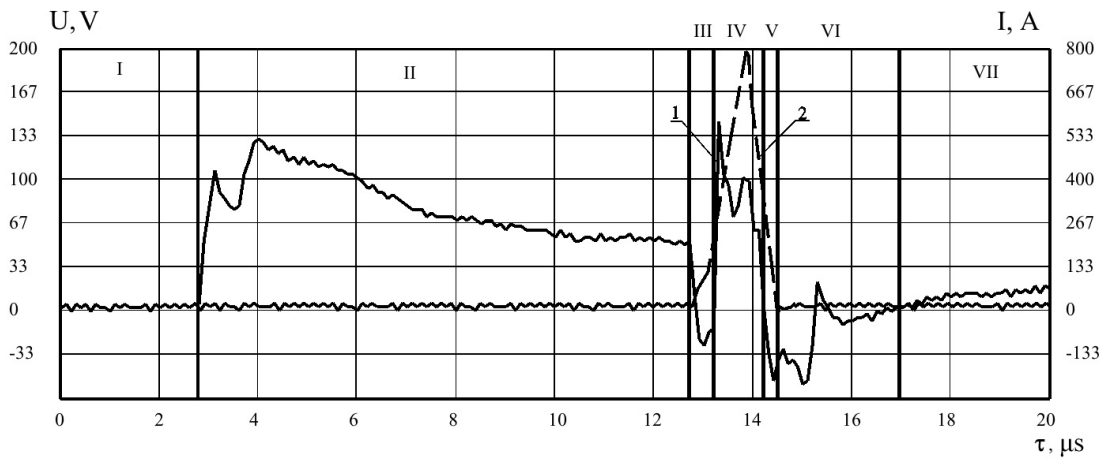

Figure 1. Oscillogram of current and voltage of a single spark discharge: 1 – voltage on the gap; 2 – discharge current; I – pause before the voltage pulse; II – gap breakdown voltage; III – determination of breakdown and switching of a powerful current source; IV – operating current pulse; V – collapse of the discharge channel; VI – electrical perturbations after discharge; VII – pause between pulses

When using AdvaCut brass wire with a diameter of 0.2 mm, to meet the technical requirements, for the vast majority of parts of aircraft and instrumentation, it is sufficient to sequentially use two, three or five passes, using the modes whose parameters are summarized in Table 1.

Table 1. Energy parameters of the most used modes of the EDM machine AccuteX GE-43SA

№	Mode code	Current pulse duration τ_i, μs	Current amplitude value I, A	Energy released at the anode, E_a, mJ	Crater diameter d, μm	The average power density in the discharge channel, q, 10^{12} W/m^2
1	NQ0024	1,2	800	28,831	101	3,03
2	NQ0018	0,9	600	13,677	80	3,06
3	NQ0014	0,7	467	7,249	66	3,07
4	NQ0010	0,5	333	3,176	52	3,05
5	NQ0007	0,35	233	1,364	41	2,95

One sample was left without EDM as a reference. The milled surfaces of five other samples are processed using the modes of the operation current generator shown in Table 1. The number of passes and the values of allowances removed on each sample are shown in Table 2 and Figure 2.

Table 2. The WEDM parameters of manufactured samples

№	Sample number	Pass number	Mode codes (Table 1)	The thickness of the layer removed per pass, μm
1	1	Without EDM		

2	2	1	NQ0024	50
3	3	1	NQ0024	50
		2	NQ0018	30
4	4	1	NQ0024	50
		2	NQ0018	30
		3	NQ0014	20
5	5	1	NQ0024	50
		2	NQ0018	30
		3	NQ0014	20
		4	NQ0010	12
6	6	1	NQ0024	50
		2	NQ0018	30
		3	NQ0014	20
		4	NQ0010	12
		5	NQ0007	5

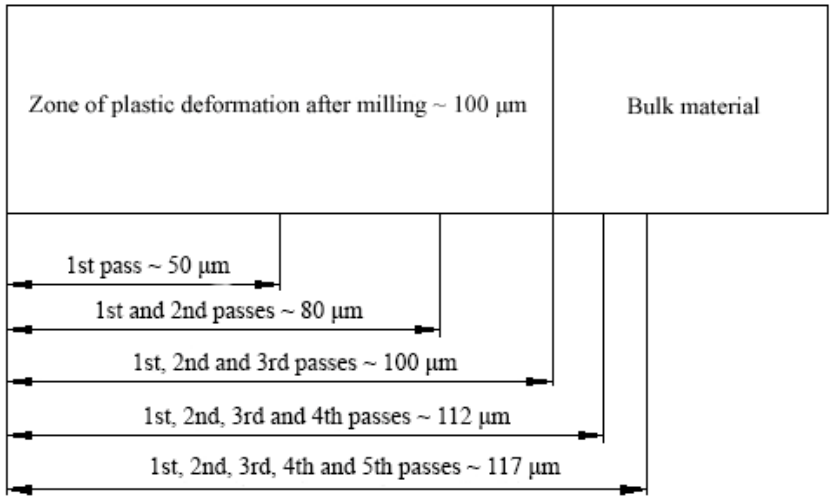

Figure 2. The layout of the surfaces formed by the multi-pass WEDM relative to the surface obtained by milling

On the formed by WEDM and obtained by milling side of the reference sample was made oblique cut by grinding. The angle of inclination for grinding the slice was determined from equation (1).

$$\alpha = arctg\frac{0.1}{100} = 0.0573° \qquad (1)$$

To obtain such an inclination during grinding, the sample was fixed in such a way that one edge of the sample rested on the plate, and the other was raised by 0.1 mm. For the convenience of further microhardness studies, 10 mm on the left side of each sample were considered “not working” and were not grinded. After forming an oblique cut to remove brittle oxides and inclusions of brass, before performing microhardness measurements, the surfaces were washed with an aqueous solution of ammonia and thoroughly wiped with hard wipes. The actual state of the surface before the study was monitored by microscopy (Fig. 5a). Microhardness measurements were performed using a hardness tester model PMT-3 and a precise coordinate table on which the workpiece was fixed and moved.

When determining the microhardness for each sample, 20 experiments were performed with a step of 1.5 mm, which corresponds to a depth step of 1.5 μm. Three measurements were performed for each experiment (Fig. 3). To increase the reliability of the obtained results, the average of the three values was determined (Table 3).

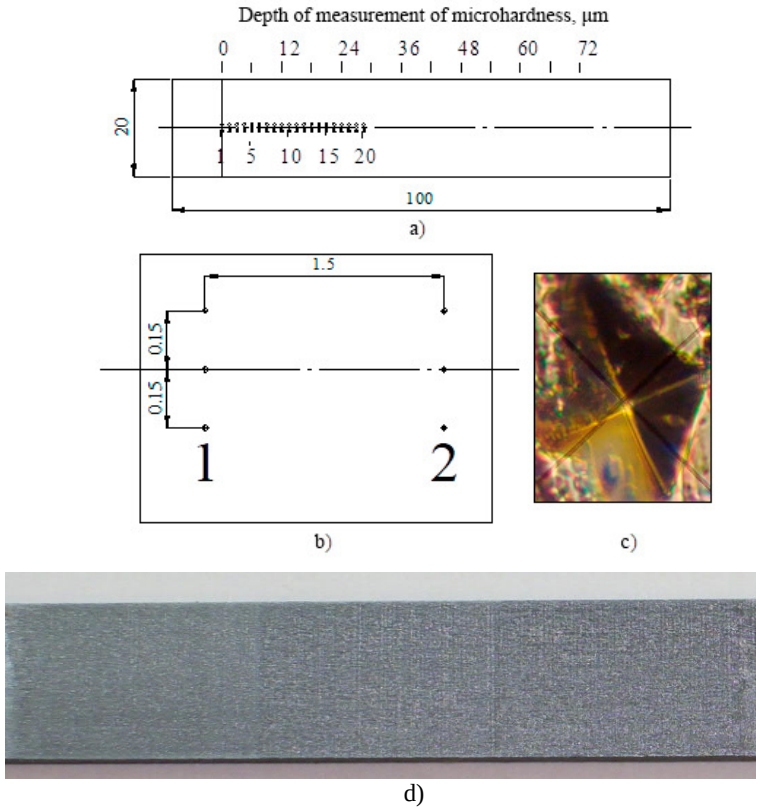

Figure 3. The scheme of studies of microhardness distribution throughout thickness of a sample: a) the general scheme of measurement; b) location of measuring points; c) an imprint of the indenter; d) the surface of the sample (×1.3) after WEDM (mode NQ0024)

3. RESULTS AND DISCUSSION

The results of microhardness studies for all samples are presented in Table 3.

Table 3. The results of experimental studies of the microhardness distribution in the thickness of the surface layers.

Studies, №	Depth of measurement, μm	Sample 1 (w/o WEDM)		Sample 2		Sample 3	
		Diagonals, mm	HV	Diagonals, mm	HV	Diagonals, mm	HV
1	0	0.0234	338.6095	0.019	513.5983	0.0175	605.4171
2	1.5	0.0233	341.5222	0.017	641.5536	0.0164	689.3553
3	3	0.0233	341.5222	0.0165	681.0248	0.0162	706.4815
4	4.5	0.0235	335.7338	0.0168	656.9196	0.0167	664.8105
5	6	0.0235	335.7338	0.0166	672.8444	0.0168	656.9196
6	7.5	0.0237	330.0913	0.0164	689.3553	0.017	641.5536
7	9	0.0235	335.7338	0.0168	656.9196	0.0295	213.0526
8	10.5	0.0234	338.6095	0.03	206.01	0.025	296.6544
9	12	0.0237	330.0913	0.0265	264.0214	0.0238	327.3233
10	13.5	0.0233	341.5222	0.0237	330.0913	0.0287	225.0956
11	15	0.0235	335.7338	0.0236	332.8946	0.0285	228.2659
12	16.5	0.0238	327.3233	0.0233	341.5222	0.0281	234.8109
13	18	0.0236	332.8946	0.0237	330.0913	0.029	220.4625
14	19.5	0.0235	335.7338	0.0238	327.3233	0.0284	229.8763
15	21	0.0235	335.7338	0.0236	332.8946	0.0288	223.5352
16	22.5	0.0234	338.6095	0.0236	332.8946	0.027	254.3333
17	24	0.0235	335.7338	0.0235	335.7338	0.0279	238.1894
18	25.5	0.0237	330.0913	0.0236	332.8946	0.0283	231.5037
19	27	0.0233	341.5222	0.0234	338.6095	0.0281	234.8109

20	28.5	0.0233	341.5222	0.0237	330.0913	0.0284	229.8763

Continuation of table 3

Studies, №	Depth of measurement, μm	Sample 4		Sample 5		Sample 6	
		Diagonals, mm	HV	Diagonals, mm	HV	Diagonals, mm	HV
1	0	0.0188	524.5841	0.0185	541.7356	0.019	513.5983
2	1.5	0.0168	656.9196	0.0165	681.0248	0.0168	656.9196
3	3	0.0168	656.9196	0.0174	612.396	0.0172	626.7205
4	4.5	0.0163	697.8396	0.0177	591.8127	0.029	220.4625
5	6	0.017	641.5536	0.0275	245.1689	0.0285	228.2659
6	7.5	0.0285	228.2659	0.0277	241.6414	0.0288	223.5352
7	9	0.029	220.4625	0.0279	238.1894	0.0284	229.8763
8	10.5	0.0294	214.5044	0.0284	229.8763	0.0289	221.9909
9	12	0.028	236.4911	0.028	236.4911	0.0292	217.4529
10	13.5	0.0287	225.0956	0.0281	234.8109	0.0287	225.0956
11	15	0.029	220.4625	0.0278	239.9061	0.0275	245.1689
12	16.5	0.0285	228.2659	0.029	220.4625	0.0279	238.1894
13	18	0.0291	218.9499	0.0286	226.6725	0.0285	228.2659
14	19.5	0.0294	214.5044	0.0284	229.8763	0.0281	234.8109
15	21	0.0284	229.8763	0.0294	214.5044	0.0286	226.6725
16	22.5	0.0288	223.5352	0.0287	225.0956	0.0289	221.9909
17	24	0.0288	223.5352	0.0285	228.2659	0.0283	231.5037
18	25.5	0.0292	217.4529	0.0291	218.9499	0.0286	226.6725
19	27	0.029	220.4625	0.0294	214.5044	0.029	220.4625
20	28.5	0.0287	225.0956	0.029	220.4625	0.0287	225.0956

For analysis convenience we presented the data from Table 3 in graphical form (Fig. 4).

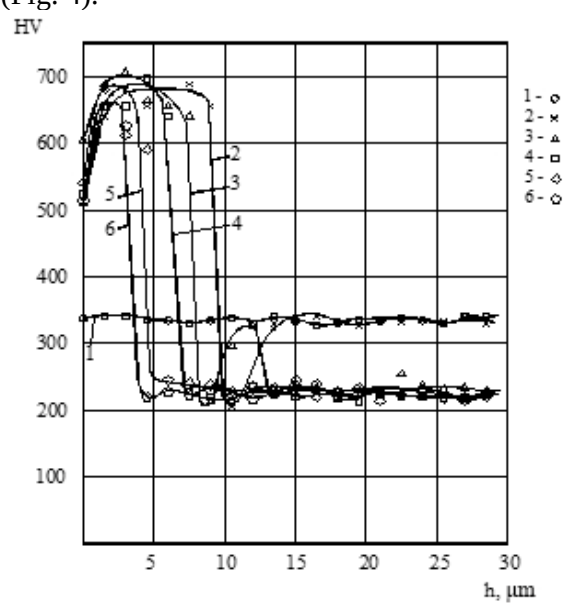

Figure 4. Distribution of microhardness throughout the depth of samples: 1 – reference sample after milling; 2-6 – samples after WEDM (Tables 2 and 3)

Curve 1 corresponds to the reference sample, which is machined only by milling. During rough milling due to significant plastic deformations, the surface hardness increases by ~ 1.3 times. Fluctuations in hardness from HV 327 to 343 (<5%) can be explained by the measurement error of the

diagonals of the imprint and a certain unevenness of the structure. In general, the surface layer can be considered homogeneous with a hardness of ~ HV335.

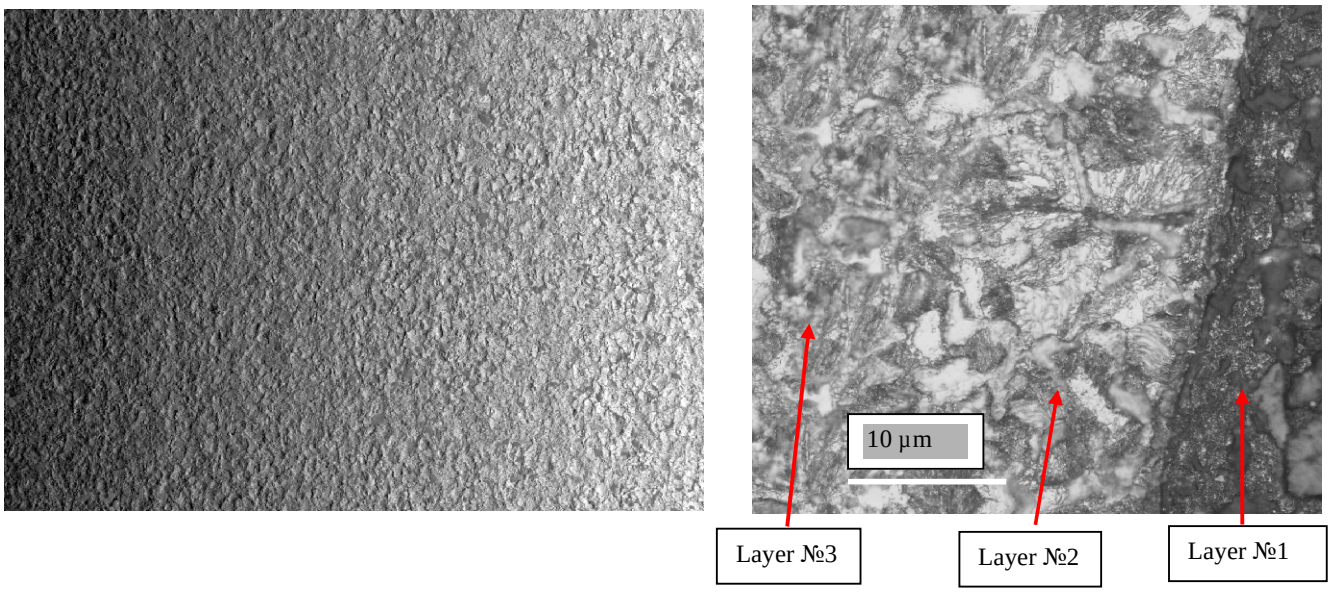

a) b)

Figure 5. Check image of the sample surface (×50), (a) before microhardness measurements (ungrinded area, mode NQ0024); (b) a cross-sectional view of sample which illustrates the thickness and structure of the surface layers after WEDM (mode NQ0024)

Curves 2-6 correspond to the multi-pass machining examples shown in Tables 1 and 2. Note that each EDM pass creates a HAZ on the surface, which is removed by the next pass or remains on the surface if the pass was the last.

Now we analyze curves 2-6. From the obtained values it is seen that in comparison with the untreated sample, the surface layers after WEDM have a thermally hardened zone. The width of this zone increases with increasing pulse duration and energy. The microhardness of the material in the thermally hardened layer is close to the hardness of martensite structures. On the surface of the samples in all cases the microhardness is less than in the next layer. This can be explained by the presence on it of a small amount of brass, which was transferred from the wire electrode and mixed with the molten material of the sample.

Curve 2, which corresponds to a single-pass EDM using mode NQ0024 (Table 1), shows that the width of the thermally hardened layer is ~ 9.5 µm. From the cross section of the sample (Fig. 5 b) it is seen that part of this layer (Layer №1) is the remelted material of the sample. Moreover, the extreme values of microhardness in this area exceed the maximum achievable with standard hardening of this grade of steel. This fact is most likely described by extremely high heating and cooling rates, unattainable in standard quenching conditions. As a result, extremely nonequilibrium structures with high heterogeneity in composition and structure are formed in the discharge zone, which give iron-carbon alloys such unique properties as ultra-high hardness. However, the issue of effective use of such secondary structures in metallurgy is not considered and the structural-kinetic approach to the study of secondary phase and structural transformations that cause a significant increase in the performance of the surface layers of steel has not been developed. It should also be noted that upon confirming the ultra-high hardness for Steel 45 in the experimental conditions, the presence of microcracks was not detected. The thickness of Layer №1 is quite stable, with a clear boundary. After Layer №1, the microhardness of the material decreases sharply to HV 206 and over the next 5 µm gradually increases to HV 335. These fluctuations in microhardness actually mean that the material at a given depth did not have time to warm up to temperatures at which martensite transformation is possible, but the relieving process took place. On the cross section it is the Layer №2 zone. Starting from a depth of 15 µm, the material is in the same state as before EDM (Layer №3). There is no clear boundary between Layer №2 and Layer №3, they overlap.

Curve 3, which corresponds to the two-pass WEDM in modes NQ0024 and NQ0018, shows that the width of the thermally hardened zone does not exceed 8 µm. Beneath this zone the material is relieved, the hardness increases, but from a depth of 13 µm the microhardness decreases to HV220. In fact, this means that at this depth is the boundary of

the plastically reinforced layer, under which the material is in the relieved state.

Curve 4 corresponds to the three-pass EDM using modes NQ0024, NQ0018, NQ0014. The thickness of the thermally hardened layer does not exceed 6 μm, after which the microhardness is reduced to HV220. In this case, the zone of plastic deformation is absent, and therefore the increase in microhardness with increasing depth in this and subsequent modes is not detected.

Curves 5 and 6 correspond to the processing in modes NQ0024, NQ0018, NQ0014, NQ0010 (for 4 passes) and NQ0024, NQ0018, NQ0014, NQ0010, NQ0007 (for 5 passes). The width of the thermally hardened layer is ~ 4 and 3 μm, respectively, below which the material is in the relieved state.

Thus, choosing the required number of EDM passes with different energy regimes, we not only gradually reduce the roughness, but also control the thickness of the thermally or plastically hardened layer on the surface of the part, which in turn affects its performance properties.

From the graphs (Fig. 3) it is seen that with increasing duration of the current pulse and the discharge energy released at the anode, the thickness of the thermally hardened zone increases. The average power density in the discharge channel in the studied range of modes does not change (Table 1). Based on the laws of physics of thermal processes of material destruction by low energy discharges and duration with medium density, power at the level of $1–3\cdot10^{12}$ W/m^2, when processing carbon steels between solid and gaseous there is always a melted zone whose temperature ranges from 1530ºC up to 2700 ºC [11], and therefore the majority of the duration of the discharge plasma channel does not interact directly with the material in the solid phase (except for the moment of breakdown). The geometric relationship between the diameter and depth of the hole [11] suggests that in the central part of the hole, the heating of the material in depth is uniform. Based on the above, we hypothesized that when using WEDM technologies for the machining of carbon steels, the dominant factors that determine the process of heat distribution in the plasma of the discharge channel zone and, accordingly, form a multilayer HAZ are the pulse duration and thermophysical characteristics of the material. The discharge energy released at the anode within the studied modes (average density, power in the discharge channel ~$3\cdot10^{12}$ W/m^2) plays a rather secondary role in the formation of the layers of the HAZ. In Fig. 6 presented the dependence of the thickness of the thermally hardened zone h_δ on the pulse duration τ_i constructed according to the obtained results.

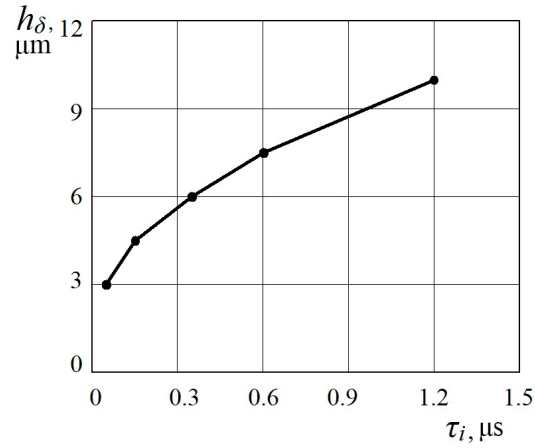

Figure 6. Dependence of the width of the thermally hardened zone on the current pulse duration (Steel 45)

If this hypothesis is true, we can assume that for WEDM of carbon steels on EDM complexes with other types of generators, the thickness of thermally hardened layers will correlate with the results presented in Figs. 6 (differences in the values of thermophysical characteristics in the group of structural and tool carbon steels do not exceed 10%).

To test the hypothesis, three additional control samples of Steel 45 were made by the same method on three other models of EDM machines on modes, the energy parameters of single pulses which are also well studied by the laboratory of electrophysical and electrochemical methods of materials processing Cherkasy State Technological University. Based on the above considerations, an EDM machine SELD-02 with a GKI-300-200 operational current generator was selected for comparison, in which the power switches are implemented on thyristors. This model was developed in the 90s of the last century, but many models of machines still work successfully at Ukrainian enterprises. The second machine was the model SELD-04 from "ARAMIS", Cherkasy with a more modern operational current generator, made on high-speed switching transistors. The third machine was the AgieCharmilles CUT 20P model from the Swiss company AgieCharmilles, which is one of the world leaders in the production of EDM machines. The energy characteristics of the modes and the results of determining the maximum thicknesses of the thermally hardened layers are shown in Table 4.

Table 4. The thickness of the HAZ after machining of Steel 45 on EDM complexes of different types

№	Manufacturer, model	Mode code	Energy released at the anode, E_a, mJ	Current amplitude value I, A	Current pulse duration τ_i, μs	Depth of thermally hardened zone h_δ, μm
1	SPE «Rotor», SELD-02	2–2	2.45	85	7.1	28
2	«Aramis», SELD-04	4	4.78	125	1.85	14
3	AgieCharmilles CUT 20P	M6	26.3	800	1.2	11

Within the obtained amount of data there is a clear correlation between the pulse duration and the thickness of the thermally hardened layer, which can no longer be stated in relation to the discharge energy in the selected range of modes. Thus, the most powerful mode with a pulse energy of 26.3 mJ, an amplitude of the operating current of 800 A, but with a pulse duration of 1.2 μs, creates a thermally hardened layer on the surface with a thickness of 11 μm, and a pulse with an energy of 2.45 mJ, but stretched in time of 7.1 μs leads to the formation of the same layer with a thickness of 28 μm. The obtained results of control researches, as a whole, serve as confirmation of the put forward hypothesis and within possible margin of errors do not contradict to the data received from the AccuteX GE-43SA EDM machine and presented in Fig. 6.

4. CONCLUSION

1. There was conducted a systematic set of studies to determine the microhardness and thickness of the thermally hardened zone in high-quality carbon structural Steel 45 after WEDM. The obtained results provide replenishment of the database and expansion of ideas about the regularities of the influence of time-energy characteristics of technological current pulses on the formation of a thermally hardened layer by WEDM of high-quality carbon steels. The possibility of effectively influencing the formation of the necessary physical and mechanical properties of the surface layers of parts made of carbon steels by the time parameters of a single spark discharge is proved.

2. In the zone of thermal hardening of Steel 45 after WEDM extreme values of microhardness which exceed the maximum achievable at standard hardening of this grade of steel are revealed. This fact is explained by extremely high heating and cooling rates, unattainable in standard quenching conditions. As a result, extremely nonequilibrium structures with high heterogeneity of composition and structure are formed in the discharge zone, which give iron-carbon alloys such unique properties as ultra-high hardness.

3. The hypothesis that in WEDM of high-quality carbon steels with the use of discharge current pulses with energy and time parameters characteristic of modern EDM machines has a dominant effect on the formation of the thickness of the thermally hardened layer has been proposed, substantiated and experimentally confirmed. The amount of discharge energy released at the anode within the parameters of the conducted experiments has a secondary effect on this process.

4. The obtained results, with a margin of error not exceeding 15%, can be used to predict the thickness of the thermally hardened layer for WEDM of a wide group of structural and tool carbon steels.

5. REFERENCES

1. Choi, K.-K., Nam, W.-J., Lee, Y.-S., Effects of heat treatment on the surface of a die steel STD11 machined by W-EDM, *Journal of materials processing technology*, Vol. 201, No. 1, pp. 580-584, (2008). https://doi.org/10.1016/j.jmatprotec.2007.11.156

2. Pop, G.I., Ţîţu, M.A., Cupşan, V.C., Nonconventional manufacturing work preparation for wire EDM machining, *Nonconventional Technologies Review*, Vol. 23, No. 2, pp. 41-46, (2019). http://www.revtn.ro/index.php/revtn/article/view/221

3. Oniszczuk, D., Świercz, R., An investigation into the impact of electrical pulse character on surface texture in the EDM and WEDM process,

Advances in Manufacturing Science and Technology, Vol. 36,No. 3, pp. 43-53, (2012). http://yadda.icm.edu.pl/baztech/element/bwmeta1.element.baztech-article-BOS6-0003-0043/c/httpadvancesmst_prz_edu_plpdfy04-oniszczuk-swiercz.pdf

4. Dhobe, M., Chopde, I., Gogte, C., Investigations on surface characteristics of heat treated tool steel after wire electro-discharge machining, *Materials and Manufacturing Processes*,Vol. 28, No. 10, pp. 1143-1146, (2013). https://doi.org/10.1080/10426914.2013.822976

5. Cao, C., Zhang, X., Zha, X., Dong, C., Surface integrity of tool steels multi-cut by wire electrical discharge machining, *Procedia Engineering*, Vol. 81, pp. 1945-1951, (2014). https://doi.org/10.1016/j.proeng.2014.10.262

6. Klocke, F., Hensgen, L., Klink, A., Ehle, L., Schwedt, A., Structure and Composition of the White Layer in the Wire-EDM Process, *Procedia CIRP*, Vol. 42, pp. 673-678, (2016). https://doi.org/10.1016/j.procir.2016.02.300

7. Schulze, H.-P., Herms, R., Juhr, H., Schaetzing, W., Wollenberg, G., Comparison of measured and simulated crater morphology for EDM, *Journal of materials processing technology*, Vol. 149, No. 1, pp. 316-322, (2004). https://doi.org/10.1016/j.jmatprotec.2004.02.016

8. Osypenko, V., Plakhotnyi, O., Timchenko, O., Surface forming features of new combined wire electrical discharge-electrochemical machining technology, *Nonconventional Technologies Review*, Vol. 23, No. 2, (2019). http://www.revtn.ro/index.php/revtn/article/view/223

9. Plakhotnyi, O., Osypenko, V., Forming and finishing surface by sequential electrochemical-electrodischarge machining of precision magnetic optics parts, *Int. J. Machining and Machinability of Materials*, Vol. 22, No. 3/4, pp. 331-347, (2020). https://doi.org/10.1504/IJMMM.2020.107061

10. Straka, L., Corny, I., Pitel, J., Properties Evaluation of Thin Microhardened Surface Layer of Tool Steel after Wire EDM, *Metals*, Vol. 6, No. 5, P. 95, (2016). https://doi.org/10.3390/met6050095

11. Osypenko, V.I., Timchenko, O.V., Kondakov, A.V., Modeling of thermal processes of a single crater formation by discharges of modern generators of EDM cutting machines, *Bulletin of Cherkasy State Technological University*, No. 3, pp. 154-162, (2019). *(In Ukrainian).* https://doi.org/10.24025/2306-4412.3.2019.182555